Hybrid Numerical Techniques for Power Transformer Modeling: A Comparative Analysis Validated by Measurements

Marina A. Tsili, Antonios G. Kladas, *Member, IEEE*, Pavlos S. Georgilakis, *Member, IEEE*, Athanasios T. Souflaris, Costas P. Pitsilis, John A. Bakopoulos, and Dimitris G. Paparigas

***Abstract*—The paper presents alternative numerical techniques implemented in power transformer analysis and design focusing on the short circuit impedance evaluation. The proposed method adopts a particular reduced scalar potential formulation enabling a three-dimensional (3-D) magnetostatic problem solution. This method, requiring no source field calculation, in conjunction with a mixed finite-element/boundary-element technique, results in a very efficient 3-D numerical model for power transformer design office use. This model is used to develop an effective computational tool, enabling the accurate transformer characteristics prediction, thus increasing its reliability and reducing its production cost. The computed results of the proposed methodology are validated through measurements in the case of a three-phase wound core power transformer.**

***Index Terms*—Boundary-element methods, finite-element methods, hybrid methods (FEM–BEM), magnetostatics, short circuit impedance, transformers.**

I. Introduction

THE process of electric utilities restructuring, privatization, and deregulation has created a competitive, global marketplace for energy. In this new and challenging environment, there is an urgent need for a transformer manufacturing industry to improve transformer efficiency and reliability and to reduce cost, since high-quality low-cost products have become the key to survival [1], [2]. Transformer reliability is improved by the accurate evaluation of the leakage field, the short circuit impedance, and the resulting forces on transformer windings under short circuit, since these enable to avoid mechanical damages and failures during short circuit tests and power system faults. The technical and economical optimization of transformer design contributes significantly in transformer cost reduction.

Numerical modeling techniques are nowadays well established for power transformer analysis and enable representation of all important features of these devices. Techniques based on finite elements present interesting advantages for nonlinear characteristics simulation. In [3]–[6], finite-element models are used for the computation of short circuit forces and leakage field evaluation in transformers. The boundary-element method is another numerical technique extensively used for electromagnetic problems. The main attraction of this method is the simplicity of the data required to solve these problems, along with the high accuracy obtained with boundary elements [7].

Moreover, the combination of boundary and finite elements is another widely used numerical field analysis technique. Three-dimensional (3-D) hybrid models for electromagnetics are introduced in [8] and [9]. Coupled finite/boundary element formulations applied on motors are also presented in [10] and [11].

In this paper, a particular reduced scalar potential formulation is adopted, necessitating no prior source field calculation in conjunction with a mixed finite-element/boundary-element technique. The accuracy of the mixed technique is investigated by comparison to the classical finite-element method for a simplified geometry. Afterwards, it is applied to a three-phase wound core power transformer and its results are compared to the respective measured ones. Finally, discussion is being made on the development of a computational tool based on this method, offering the possibility of generalization of its application.

II. Modeling Techniques

A. Finite-Element Method (FEM)

The FEM is a numerical technique for the solution of problems described by partial differential equations. The governing equation in the case of a magnetostatic field is the Laplace equation

$$\nabla^2 \Phi_m = 0 \tag{1}$$

where Φ_m is the scalar magnetic potential. The considered field is represented by a group of finite elements. Therefore, a continuous physical problem is converted into a discrete problem of finite elements with unknown field values in their vertices nodes.

Many scalar potential formulations have been developed for 3-D magnetostatics, but they usually necessitate a prior source field calculation by using Biot–Savart's law. This presents the drawback of considerable computational effort.

In the present paper a particular scalar potential formulation has been developed, enabling the 3-D magnetostatic field analysis. According to our method the magnetic field strength H is

Manuscript received July 1, 2003. This work was supported in part by the General Secretariat for Research and Technology of Greece under PAVET Grant 00BE457.

M. A. Tsili and A. G. Kladas are with the Faculty of Electrical and Computer Engineering, National Technical University of Athens, GR-15780 Athens, Greece (e-mail: kladasel@central.ntua.gr).

P. S. Georgilakis, A. T. Souflaris, C. P. Pitsilis, J. A. Bakopoulos, and D. G. Paparigas are with Schneider Electric SA, Elvim Plant, GR-32011 Inofyta, Viotia, Greece (e-mail: dimitris_paparigas@mail.schneider.fr).

Digital Object Identifier 10.1109/TMAG.2004.825303

conveniently partitioned to a rotational and an irrotational part as follows:

$$\mathbf{H} = \mathbf{K} - \nabla\Phi \tag{2}$$

where Φ is a scalar potential extended all over the solution domain while $\mathbf{K}$ is a vector quantity (fictitious field distribution), that satisfies the following conditions [12]:

1) $\mathbf{K}$ is limited in a simply connected subdomain comprising the conductor;
2) $\nabla\mathbf{x}\mathbf{K} = \mathbf{J}$ in the conductor and $\nabla\mathbf{x}\mathbf{K} = 0$ outside it;
3) $\mathbf{K}$ is perpendicular on the subdomain boundary.

The above formulation satisfies Ampere's law for an arbitrary contour in the subdomain.

B. Boundary-Element Method (BEM)

The BEM is derived through discretization of an integral equation that is mathematically equivalent to the original partial differential equation. The boundary integral equation corresponding to Laplace equation is of the form

$$c(s)\Phi(s) + \oint_{\Gamma}\left[\Phi(s)\frac{\partial G(s',s)}{\partial n} - G(s',s)\frac{\partial\Phi(s')}{\partial n'}\right]ds' = 0 \tag{3}$$

where s is the observation point, s' is the boundary Γ coordinate, n' is the unit normal, and G the fundamental solution of Laplace equation in free space. While in the FEM an entire domain mesh is required, in the BEM formulation a mesh of the boundary only is required, resulting in the significant reduction of the problem size.

C. Mixed FEM–BEM

Another field analysis method can be derived by the above two mentioned techniques. With the use of this method, problems with geometries comprising large parts of air can be solved by a reduced discretization through boundary elements in combination with the ability of better representation of nonlinear materials provided by the FEM.

Let us consider a 3-D coupled finite-element/boundary-element solution domain, comprising m finite-element nodes, n boundary-element nodes, and k common nodes at the interface boundary. The total number of nodes is equal to N, where

$$N = m + n - k. \tag{4}$$

The finite-element mesh consists of i_{FEM} tetrahedra while the boundary-element mesh comprises i_{BEM} triangles. The matrix form of the equations corresponding to the above solution domain is of the form of (5) [5], [6] where Φ_i and $(\partial\Phi_i/\partial n)$ are the nodal potential and nodal potential derivative values of the node i, respectively.

The left-hand matrix of (5) consists of five "submatrices": [S], [F], [G], [H], and [T] which are described in the following:

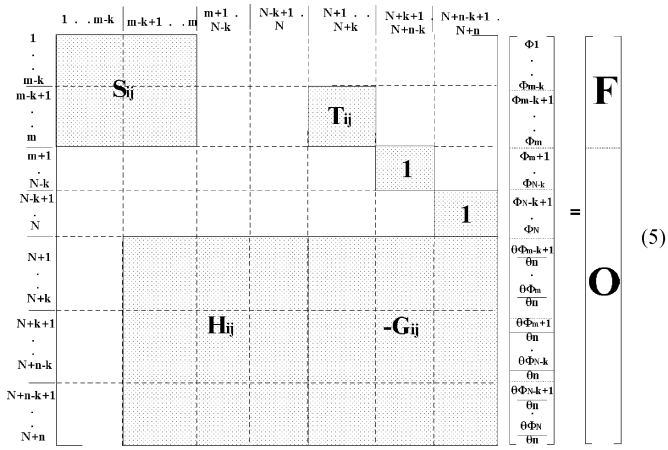

(5)

[S] is the stiffness matrix and [F] the source vector of the FEM corresponding to (6)

$$[\mathrm{S}][\Phi] = [\mathrm{F}]. \tag{6}$$

The general form of their elements is

$$S_{ij} = \int_{S_{\mathrm{element}}} \nabla a_i a_j dS \tag{7}$$

$$F_i = \int_{S_{\mathrm{element}}} a_i \vec{K}_i dS. \tag{8}$$

[H] and [G] are the matrices of the boundary-element method. The general form of their elements is

$$H_{ij} = \begin{cases} \oint_{\Gamma_j} \frac{\partial G_i(s',s)}{\partial n} ds', & i \neq j \\ c_i, & i = j \end{cases} \tag{9}$$

$$G_{ij} = \oint_{\Gamma_j} G_i(s',s) ds'. \tag{10}$$

[T] is the matrix of the terms used to link the finite-element region to the boundary-element region (involving the potential and normal derivative values of the FEM–BEM interface boundary nodes)

$$T_{ij} = \int_{S_{\mathrm{element}}} a_i a_j dS. \tag{11}$$

According to the above formulation, the magnetic field sources are located in the finite-element region ($F_i, 1 \leq i \leq m$). Therefore, they can be represented by the adoption of the vector quantity $\mathbf{K}$ described previously. On the other hand, the boundary-element region does not comprise magnetic field sources; therefore, there is no need to implement the vector field $\mathbf{K}$ in the BEM formulations.

The unit diagonal terms appearing between rows $m+1$ and N of the left-hand side matrix of (5) correspond to the imposed boundary conditions of the problem. They imply that the value of the potential derivative of the respective nodes is known. Similar assumptions can be made for the nodal potential values (according to the nature of the problem considered) by moving the columns of the diagonal terms.

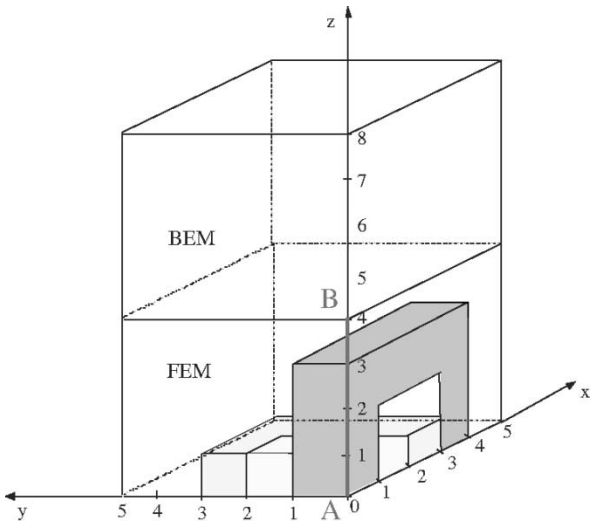

Fig. 1. Geometry of the problem considered.

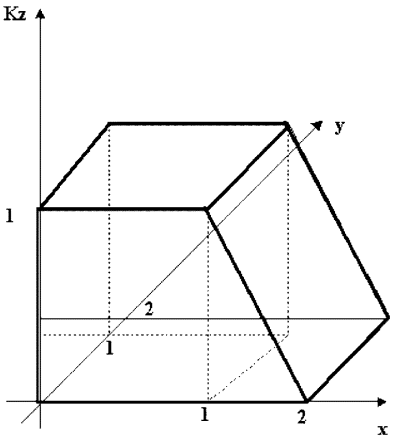

Fig. 2. Fictitious field distribution corresponding to the first coil of Fig. 1.

III. Results and Discussion

A. Investigation of the Proposed Method Accuracy in Case of a Simplified Configuration

The proposed mixed technique has been applied to the problem of Fig. 1. It consists of an iron core surrounded by two coils. This simplified configuration approximates the transformer magnetostatic field under short circuit conditions. The solution domain is reduced to one eighth of the device and is divided into two regions: the finite-element region, which comprises the iron core part and the coils, and the boundary-element region which represents the air surrounding the active part. The symmetries of the problem were taken into consideration by the imposition of Dirichlet boundary condition ($\Phi = 0$) along x–y plane and Neumann boundary condition ($\partial\Phi/\partial n = 0$) along the other outer three faces.

The mixed FEM–BEM mesh consists of 276 nodes: 180 in the finite-element region, 132 in the boundary-element region, and 36 in the interface boundary (plane $z = 4$). The FEM mesh is composed of 600 tetrahedra and the BEM region of 260 triangles.

Fig. 2 shows the distribution of the fictitious field distribution $\mathbf{K}$ corresponding to the first coil of Fig. 1.

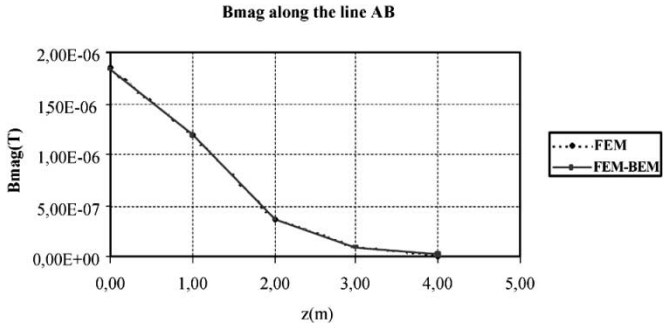

Fig. 3. Variation of magnetic induction magnitude along line AB of Fig. 1.

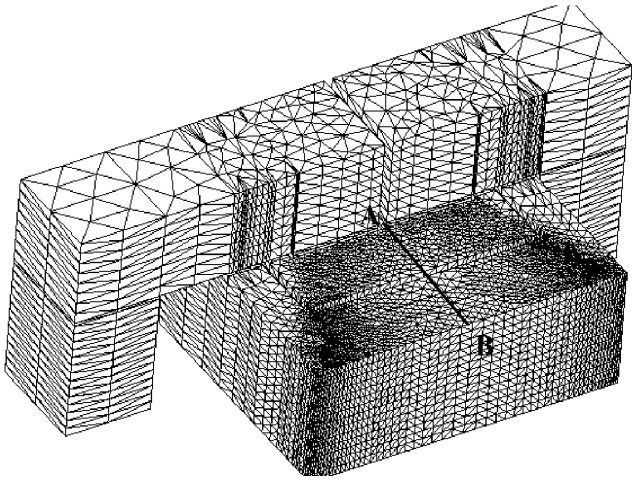

Fig. 4. Tetrahedral finite-element mesh representing the transformer active part.

In order to check the accuracy of the proposed mixed technique, the same problem was solved with the use of only FEM. The respective 3-D FEM mesh adopted, consists of 360 nodes and 1200 tetrahedra. Fig. 3 compares the magnetic induction magnitude variation along the line AB of Fig. 1 as it was calculated by the two methods. The results are in very good agreement.

B. Application of the Proposed Method to a Real Transformer Case—Experimental Validation

The proposed method has also been applied in the 3-D numerical analysis of a transformer under short circuit for its leakage reactance calculation. The case of the one phase part of a 630 kVA, rated primary voltage 20 and 15 kV (dual voltage in primary winding), rated secondary voltage 400 V, three-phase, wound core, power transformer, has been considered. Fig. 4 illustrates the perspective view of the one-phase transformer part modeled as well as the corresponding finite-element mesh. This mesh is considerably more dense in the windings area in order to obtain greater accuracy in the magnetic field sources region.

The field values computed by the proposed 3-D formulation have been compared to those measured by a Hall effect probe during short circuit test. Fig. 5 and 6 give the variation of the perpendicular flux density component B_n along the line AB, positioned as shown in Fig. 4, in case of short circuit with the high-voltage winding connections corresponding to 20 and

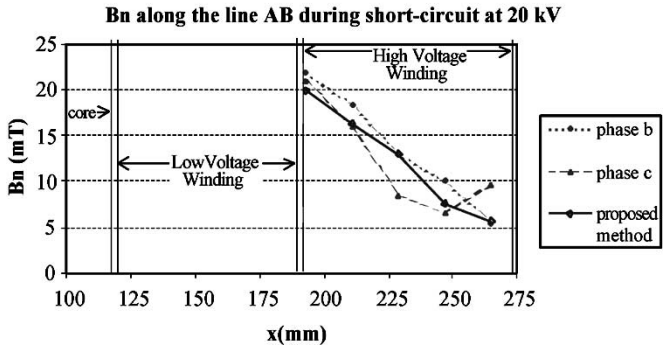

Fig. 5. Comparison of measured and computed field values along the line AB during short circuit at 20 kV.

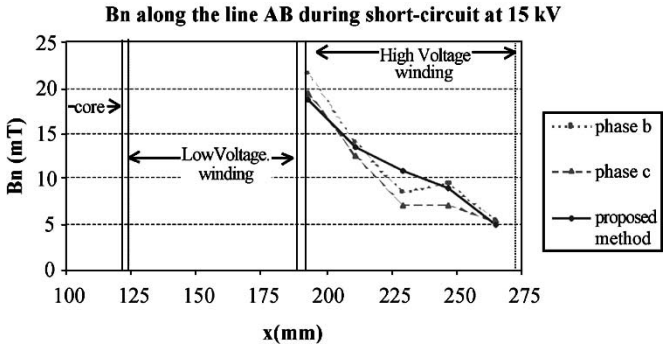

Fig. 6. Comparison of measured and computed field values along the line AB during short circuit at 15 kV.

TABLE I
COMPARISON OF MEASURED AND COMPUTED SHORT CIRCUIT IMPEDANCE VALUES

Primary Voltage Level	Measured Value	Calculated Value	Difference (%)
20 kV	5,61	5,73	2,13
15 kV	5,50	5,62	2,18

15 kV voltage supply. These figures illustrate the good correlation of the simulated results with the local leakage field measurements.

The measured short circuit impedance deduced by this test was compared to the one calculated with the use of the proposed method. The results and the respective deviation appear in Table I. The measured and calculated values are very close for both voltage levels, with similar difference less than 2.2%.

C. Generalization of Results

The proposed methodology has been adopted in the development of a computer code which implements the short circuit impedance calculation for three-phase dual voltage wound core transformers. This tool has been used during the design of transformers with different power ratings and voltage levels in the primary winding. Table II lists the calculated short circuit impedance values in three cases along with the ones measured after the construction. The respective difference is less than 2.7%, while in some cases it reduces to less than 0.5%.

TABLE II
APPLICATION OF THE PROPOSED METHOD TO SEVERAL TRANSFORMER CASES

	Rating	Primary Voltage Level	Measured Value	Calculated Value	Difference (%)
1	*1000*	*20 kV*	6,27	6,26	0,16
	kVA	*15 kV*	6,17	6,30	2,11
2	*630*	*20 kV*	3,77	3,83	1,59
	kVA	*6,6 kV*	3,75	3,81	1,60
3	*100*	*20 kV*	4,16	4,27	2,64
	kVA	*15 kV*	4,17	4,19	0,48

IV. CONCLUSION

The paper introduced a 3-D mixed finite-element/boundary-element model for three-phase, wound core, dual voltage, power transformers. The method is based on a particular reduced scalar potential technique necessitating no source field calculation. The results of the proposed methodology have been validated through local leakage field measurements and checked in several power transformer cases. The relevance between measured and computed values render this hybrid numerical technique a powerful computational tool for transformer short circuit impedance evaluation.

REFERENCES

[1] P. S. Georgilakis, N. D. Doulamis, A. D. Doulamis, N. D. Hatziargyriou, and S. D. Kollias, "A novel iron loss reduction technique for distribution transformers based on a combined genetic algorithm-neural network approach," *IEEE Trans. Syst., Man, Cybern. C*, vol. 31, pp. 16–34, Feb. 2001.

[2] P. Georgilakis, N. Hatziargyriou, and D. Paparigas, "AI helps reduce transformer iron losses," *IEEE Comput. Appl. Power*, vol. 12, no. 4, pp. 41–46, 1999.

[3] S. Salon, B. LaMattina, and K. Sivasubramaniam, "Comparison of assumptions in calculation of short circuit forces in transformers," *IEEE Trans. Magn.*, vol. 36, pp. 3521–3523, Sept. 2000.

[4] C. Xiang, Y. Jinsha, Z. Guoquiang, Z. Yuanlu, and H. Qifan, "Analysis of leakage magnetic problems in shell-form power transformer," *IEEE Trans. Magn.*, vol. 33, pp. 2049–2051, Mar. 1997.

[5] I. L. Nahas, B. Szabados, R. D. Findlay, M. Poloujadoff, S. Lee, P. Burke, and D. Perco, "Three dimensional flux calculation on a three-phase transformer," *IEEE Trans. Power Delivery*, vol. 1, pp. 156–160, July 1986.

[6] A. G. Kladas, M. P. Papadopoulos, and J. A. Tegopoulos, "Leakage flux and force calculation on power transformer windings under short-circuit: 2D and 3D models based on the theory of images and the finite element method compared to measurements," *IEEE Trans. Magn.*, vol. 30, pp. 3487–3490, Sept. 1994.

[7] C. A. Brebbia and R. Magureanu, "The boundary element method for electromagnetic problems," *Eng. Anal.*, vol. 4, no. 4, pp. 178–185, 1987.

[8] G. Meunier, J. L. Coulomb, S. J. Salon, and L. Krahenbul, "Hybrid finite element boundary element solutions for three dimensional scalar potential problems," *IEEE Trans. Magn.*, vol. 22, pp. 1040–1042, Sept. 1986.

[9] S. J. Salon and J. D'Angelo, "Applications of the hybrid finite element—boundary element method in electromagnetics," *IEEE Trans. Magn.*, vol. 24, pp. 80–85, Jan. 1988.

[10] M. Kuhn, "The application of coupled FE/BE formulation in technical magnetic field computations," *Comput. Methods Appl. Mech. Eng.*, vol. 157, pp. 193–204, 1998.

[11] L. Pichon and A. Razek, "Force calculation in axisymmetric induction devices using a hybrid FEM–BEM technique," *IEEE Trans. Magn.*, vol. 26, pp. 1050–1053, Mar. 1990.

[12] A. Kladas and J. Tegopoulos, "A new scalar potential formulation for 3D magnetostatics necessitating no source field calculation," *IEEE Trans. Magn.*, vol. 28, pp. 1103–1106, 1992.